High-Resolution Acoustic Imaging ILI: Introducing Triple-threat Detection and Sizing in a Single Pass

C. Richards[1], G. Simpson[1], C. Costa[1], A. Schwing[2], J. Moritz[2]
[1]DarkVision, [2]Flint Hills Resources

PPIM 2025
PIPELINE PIGGING & INTEGRITY MANAGEMENT
JANUARY 27-31 • HOUSTON

Organized by

CLARION
TECHNICAL CONFERENCES

Abstract

Pipeline operators are posed to gain significantly more intuitive results with a novel In-line Inspection tool that has been shown to be able to evaluate every major anomaly type - metal loss, axial cracks, and dents – in a single run. This technology represents a fundamental improvement in resolution and imaging techniques giving the ability to understand combined threats impacting pipelines. Direct 3D measurements reveal the shape and orientation of anomalies that enable operators to better understand the root cause and more accurately deploy risk mitigation techniques. This direct imaging method overcomes legacy amplitude-based inferred measurement methods that have limitations when measuring anomaly morphologies.

The tool leverages the latest developments from phased array in-ditch based handheld systems, medical imaging, and upstream oil and gas ultrasound imaging technologies to bring ultra-high-resolution spatial measurements at 0.5mm axial resolution and 0.25mm circumferential resolution at line speeds exceeding 2 meters/second. Over 6,000 array based independent sensors mounted on encoded carriers detect and size metal loss, axial cracks, and dent information from a single inspection.

This paper presents the validation of the technology in accordance with API 1163 best practices. A continuous flow loop was engineered and constructed to test the tool's endurance and validate the tool's performance over a variety of anomalies including electrical discharge machined (EDM) notches, manufactured cracks, natural cracks, and wall loss. These results are validated against industry standard tools including a metrology-grade laser scanner and a phased-array ultrasound handheld tool.

Lastly, findings from a full-scale deployment in a segment of Flint Hills Resources 16" transmission pipeline are summarized.

Introduction

In-line inspection technologies have evolved significantly over the decades, driven by continuous advancements in onboard electronics hardware, cloud-based machine learning algorithms, and data processing techniques. These improvements have enabled the detection of a broader range of anomalies and the precise sizing of smaller and more complex defects. This evolution has enhanced operators' ability to improve the safety and reliability of their assets. However, operators have often needed to prioritize multiple inspections with different tools to detect and inspect a wide range of anomalies and defects. This approach risks reliance on prior knowledge or assumptions about potential issues, often resulting in erroneous digs and ongoing integrity management challenges. Deploying a single high-resolution high-performance tool that exceeds the combined inspection capabilities of multiple tools offers key advantages:

- **Streamlined Operational Logistics:** Fewer tool launch and receive operations results in less time and resources required for line preparation and run operations

- **No Reduction in Line Speed or Throughput:** A tool capable of running at higher line speeds while maintaining full resolution can translate into significant value by avoid slowing the flow of product and.

- **Holistic Repair Planning:** A more comprehensive analysis of all defects, inclusive of axial cracks, metal loss, and dents, means that repairs can be better prioritized and planned more efficiently.

- **Understand Complex and Interacting Defects**: The full characteristics of a defect are contained in one dataset as all its properties from length, width, depth, displacement or geometry, and axial discontinuities are all measured from a singular technology.

- **Intuitive Insight into Defects:** High-resolution direct measurements of a defect enable contextual understanding of the shape, and contoured profile of the defect similar to advanced NDE methods and provides a higher confidence assessment beyond the reported boxed length, width, and depth size reported.

- **Higher-Quality Inspections:** Smaller and shorter defects and a wider range of defects missed by other tools are detected due to the more sensitive detection threshold and sizing capabilities of the singular high-performance tool.

This paper details the implementation and application of high-resolution acoustic imaging technology through Inline Inspection (ILI). By utilizing direct spatial measurement techniques, the technology addresses the challenges faced by existing tools and methods. It evaluates the advantages of high-resolution acoustic imaging-based methods over traditional and amplitude-based inferred detection and sizing techniques, especially in assessing wall loss, crack-like anomalies, and complex or interacting anomalies.

The Need for High-Resolution Acoustic Imaging

Most ILI technologies today rely on inferring the size of defects by correlating the amplitude of a signal to a lab-determined reference pattern to interpret how the signal correlates to a defect of a particular size.

- Magnetic flux leakage (MFL) is an indirect method for measuring wall loss, correlating the volume of metal lost to the detected flux leakage based on calibration data. Where defects get complex, interacting or close to the limits of resolution, it can be particularly challenging for this technology to provide accurate anomaly dimensions and geometry.

- Ultrasound based crack tools utilize indirect crack sizing measurements which correlate an amplitude-based response to crack depth based on lab calibration. This calibration is typically completed using idealized perfect-reflector notches in the lab which are not highly representative of the true morphology, tilt, skew or weld-seam interaction that real-world cracks encompass.

These amplitude-based sizing techniques are limited in accurately sizing and identifying complex defects, defects beyond standard thresholds, and interacting defects. Additionally, indirect measurement systems do not provide clear images of defects, leading to a strong dependence on highly skilled analysis, which can impact repeatability. Consequently, the interpretation of results often leaves room for subjective analysis, highlighting the need for further innovation and refinement in this field.

Acoustic Imaging ILI

Acoustic imaging in ILI is implemented through array-based probes mounted on independently suspended and encoded carriers. Each probe applies time delays that generate steered waves including perpendicular, clockwise, and counterclockwise wavefronts that bend into the steel at the fluid-pipe boundary. By controlling the wavefront electronically, the technology can index through transmit modes and screens for multiple threats without the need for multiple tools or multiple hardware configurations; the tool is entirely electronically configured. This approach takes full advantage of the capabilities of the phased array ultrasonic probes and results in 0.5mm axial resolution and 0.25mm circumferential resolution at a speed of over 2m/s. Each element is recorded in full raw A-scan channel data format and results in datasets which reach into petabytes of data once uncompressed and beamformed. For the 16-inch platform discussed in this paper, over 6,000 elements are independently controlled. Each element functions as an entirely independent channel without any grouping, averaging, or use of sub-apertures. This approach contrasts with the use of sub-apertures or grouped virtual sensors which throttle the resolution by operating the tool in a manner that closely resembles single-element ultrasonic (UT) tools. The singular raw dataset captured is then analyzed post-run through a combination of imaging modes to directly measure the specific surface boundaries and geometry of anomalies and defects for metal loss, cracks, and deformations in a pipeline.

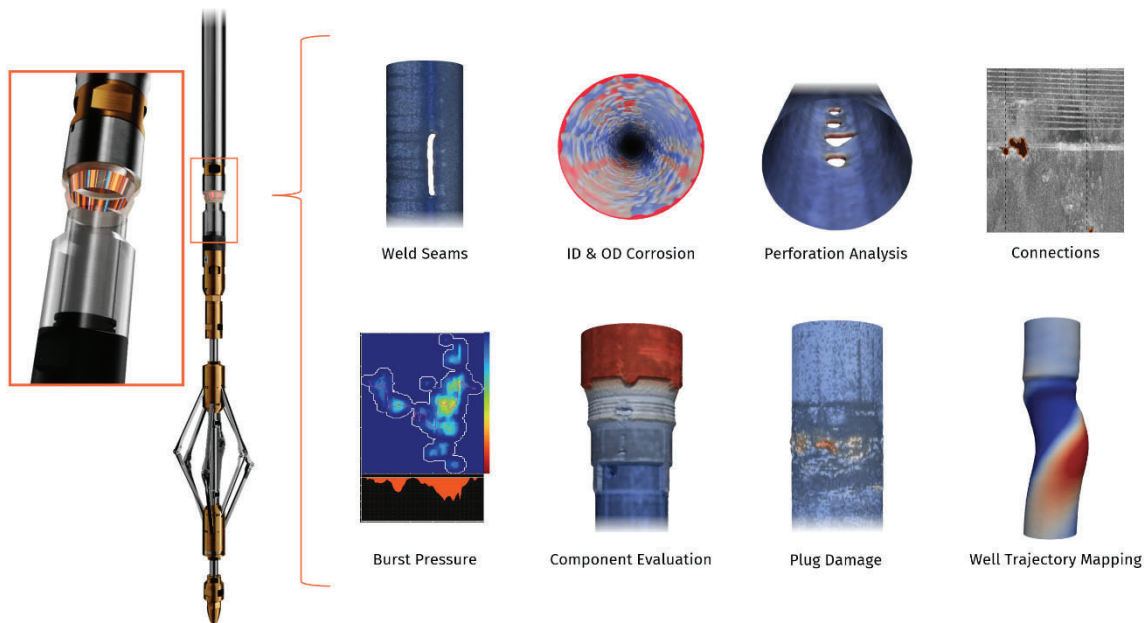**Figure 1:** High-resolution Acoustic Imaging is deployed in pipelines using a multi-body inspection tool.

The main 3 modules of the configurable system as depicted in **Figure 1** from left to right are:
1. Electronics, Navigation and Odometer module with Inertial Measuring Unit (IMU)
2. Primary cell battery module
3. Acoustic Imaging Sensor Module

The tool's mechanical chassis was designed to maximize imaging capabilities across both nominal pipe ID and changes in pipe geometry associated with dents, ovality, and deformations. The physical design of the tool ensures that each imaging probe remains in its ideal imaging position relative to the pipe wall and captures the full ID and OD profile of the wall surface over geometry changes and the full profile of dents and coincident and complex interacting threats. This also enables the tool to have a very high collapse factor to pass through restrictions.

Acoustic Imaging in Other Industries

Initially introduced by Robinson et al. (2020), High-Resolution Acoustic Imaging has been widely adopted by operators globally to investigate various well integrity and completion optimization objectives owing to its 0.01-inch resolution, direct measurements, fluid-agnostic imaging capabilities combined with rapid turnaround times and robust cloud-based inspection and analysis. The technology has been used in thousands of field runs, and has been featured in over 47 industry papers.


Figure 2: High-Resolution Acoustic Imaging in an upstream tool measures casing and tubing to assess for wall loss defects, breaches, deformation, threaded connection makeup, and completions hardware.

Direct Spatial Measurements

High-Resolution Acoustic Imaging uses direct measurement techniques to capture spatially registered high-resolution 3D point clouds of data. Originating from advanced medical and industrial Non-Destructive Evaluation (NDE) techniques, High-Resolution Acoustic Imaging captures measurements in 3D space that can be visualized to create photorealistic images and spatially accurate renderings which are more intuitive to interpret for operators and analysts. By treating each sensor in the array as a standalone element, the technology is much more capable of resolving and mapping each component of the reflected energy to a precise location within the pipe wall to a specific feature of an anomaly – what was previously seen as a noisy amplitude signal of a crack through fixed-angle pitch-catch elements is now seen and triangulated through hundreds of amplitudes returns, each with unique arrival times. The arrival times and amplitudes are spatially mapped to the defect and provide insight into the morphology, dimensions, and in some cases the root cause of the defect.

Waves are electronically steered and transmitted at different angles to enable multiple imaging modes to be applied post-run to directly detect and size various defects.

1. For sizing defects such as cracks, inclusions, and lack-of-fusion (LoF), it is advantageous to emit diverging waves that impinge on the ID of the pipe at an angle which creates shear waves (Left, cyan-blue in figure below) that propagates in the pipe wall.

2. For sizing defects such as corrosion, pitting, delamination, porosity, lack of penetration, and weld misalignment, it is advantageous to transmit diverging waves so that they impinge normally on the ID of the pipe.
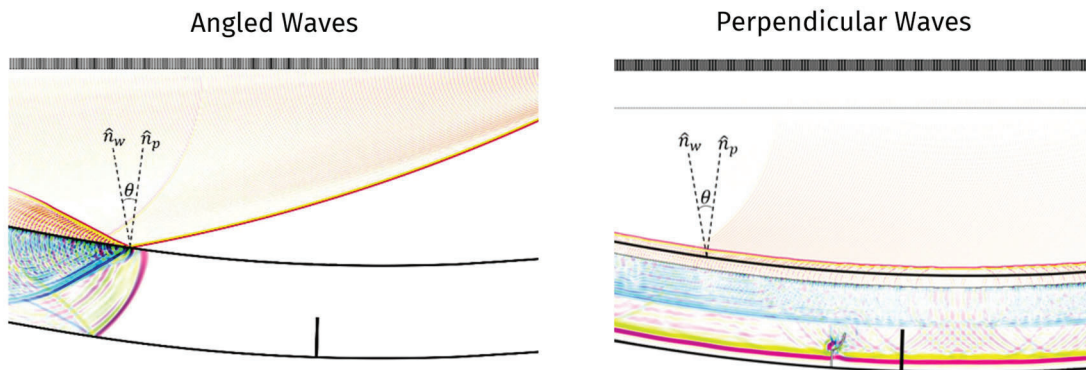
Figure 3: The tool generates clockwise and counterclockwise angled diverging wavefront (yellow-red) to create a shear wave (Left, cyan-blue) in the pipe wall and a longitudinal wave (Right) that is perpendicular to the pipe wall to maximize the detection and sizing ability of the imaging modes applied post-run.

A combination of imaging modes is applied post-run to the same dataset to extract increasing levels of information. Different imaging modes account for the summation of signal, and multiple

reflections from material boundaries in different ways, even assessing the lack of signal, and are combined to provide operators comprehensive insight into the root cause of the defect. Multiple imaging modes as depicted in **Figure 4** are combined to collectively create the results of Acoustic Imaging.
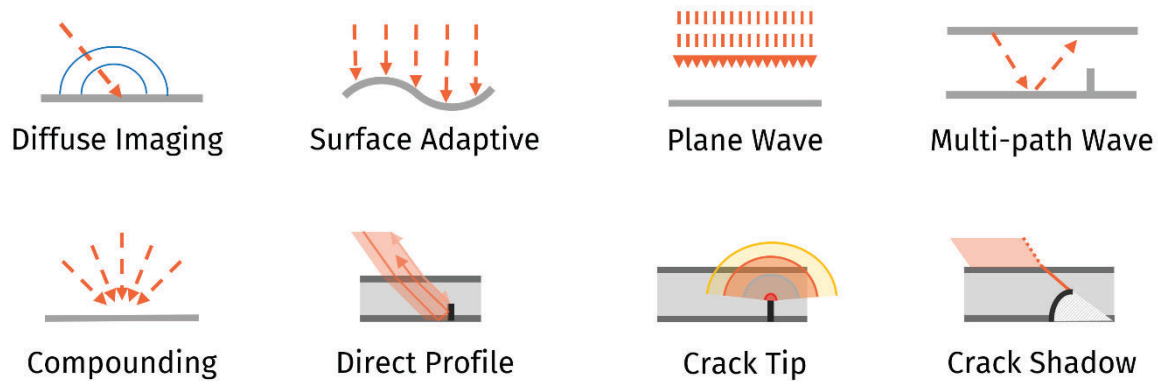
Figure 4: Various imaging modes are used to extract different information of each defect.

These different imaging modes are all direct spatial measurement techniques grounded in fundamental ultrasound principles, such as time-of-flight and speed of sound in fluid and steel layers. These methods have been shown to be more accurate than traditional amplitude-based inferred sizing practices for crack flaws. Since these imaging modes use the same raw dataset, the combined results and insights from each mode are perfectly aligned and synchronized – each imaging mode is super positioned with one another. Additionally, as these imaging modes are applied post-run to raw data, runs can be re-analyzed with more advanced methods in the future as new increasingly sophisticated imaging modes are developed.

A large-scale cloud-based computing and machine learning framework was developed to process the extensive data sets generated by this technology. By applying various imaging modes to billions of ultrasound frames, the system produces petabytes of integrity datasets. This workflow ensures results are consistent and repeatable, eliminating the need for subjective interpretation. Noteworthy imaging modes applied to specific anomaly types, and their advantages are detailed further in this paper.

## Evaluating Metal Loss Defects with Acoustic Imaging

Traditional ILI inspection methods to measure pipe wall loss are either limited in resolution with discrete single-element UT probes or are inferred-based MFL measurements. Small but critical defect features like pitting, pinholes, such as microbial-based pitting have been difficult to detect with these methods. The size of these defects is often smaller than the beam size of a single-element UT probe or fall below the resolving abilities of MFL tools. These defects are now being clearly resolved and measured with Acoustic Imaging as seen in **Figure 5** and **Figure 6.**

Diffuse Imaging – Acoustic Spatial Intensity Views

All surfaces contain varying levels of roughness. When an acoustic wave contacts a material boundary, part of the energy is scattered and reflected due to the surface roughness and imperfections - Diffuse Imaging takes advantage of this property and maps the profile of the surface from the corresponding reflections. **Figure 7** illustrates this principle. Due to the high-density nature of the point cloud measurements from High-Resolution Acoustic Imaging, it is advantageous to plot the intensity of signal returns over the length and width of the scanned area. The Acoustic Intensity view provides a high-resolution texture map of the ID and OD wall surface which can be used to further understand anomalies and provide contextual information that is valuable to understand the surrounding inner and outer surface condition at anomalies. **Figure 5**, 2nd right column of images are examples of these Acoustic Intensity views.
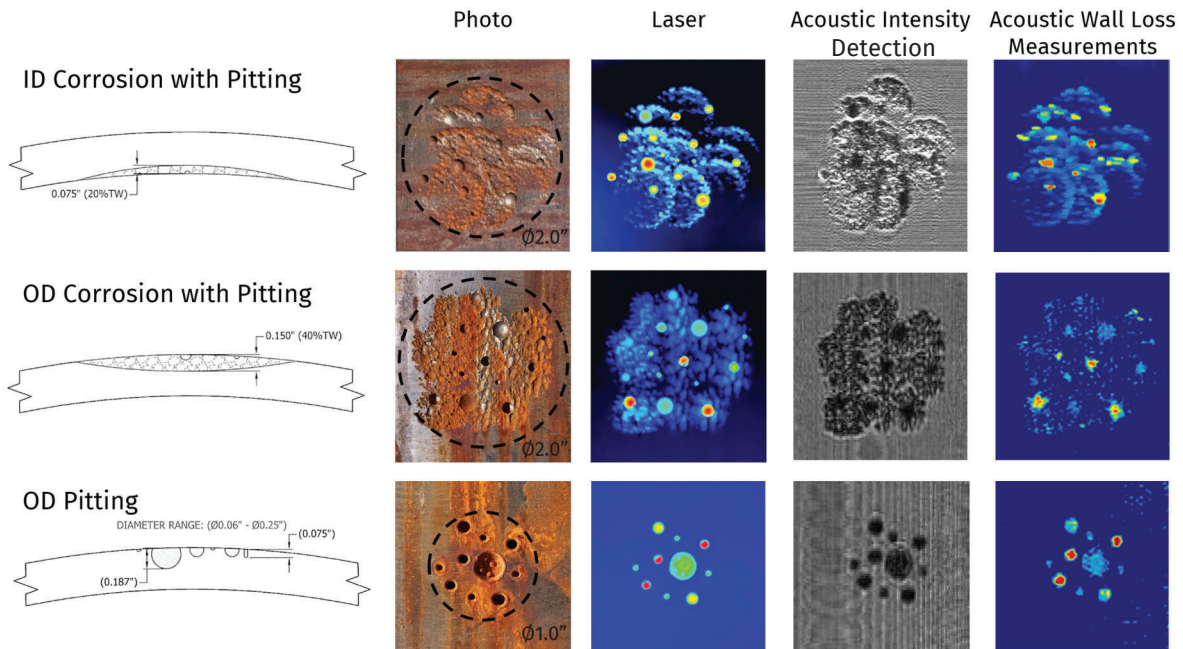
Figure 5: OD and ID pitting and corrosion is evaluated with Acoustic Imaging and compared against external laser scans. Acoustic Intensity view (2nd right) shows pipe wall surface texture.
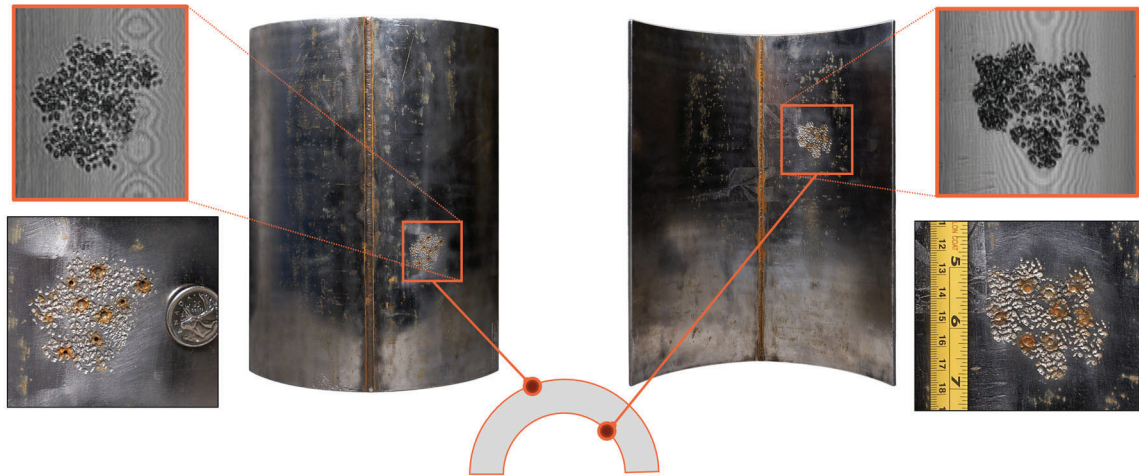
Figure 6: Acoustic Intensity Maps Generate Photorealistic Imagery of wall loss defects on the ID and OD. These maps are a useful tool for the detection and root cause analysis of defects, particularly when partnered with encompassing wall loss measurements.

Metal Loss Acoustic Imaging Modes

Pipe thickness and wall loss measurements are critical for assessing pipeline integrity. Traditional perpendicular single-element UT probe-based ILI tools rely on measuring the stand-off and time-of-flight of the transmit and return signal to identify and size defects on the ID and OD. Normally, incident transmits reflect off material boundary changes and creates regular reverberations from which thickness and wall-loss measurements can be taken, akin to an ultrasonic thickness gauge. This method is sensitive to tool dynamics and signal alignment, where changes in pipe geometry can cause echo loss such as when traveling over girth welds. Additionally, these tools struggle at the limits of their resolution particularly when the defect is natural in shape and morphology.

Acoustic Imaging leverages the fact that it sees each defect from multiple unique perspectives to directly measure the exact contour of the wall loss or the morphology of defects – resolving the edges of both sharp and deep wall loss profiles, by synthesizing images from the direct and angled transmits this approach is more likely to get acoustic energy to the defect and record a responding reflection. This imaging mode is referred to as diffuse imaging and is particularly differentiated at imaging ID wall loss defects. **Figure 7** exemplifies these capabilities. This makes it possible to differentiate between pitting, corrosion, denting, weld misalignment and other defects which have differing shapess.
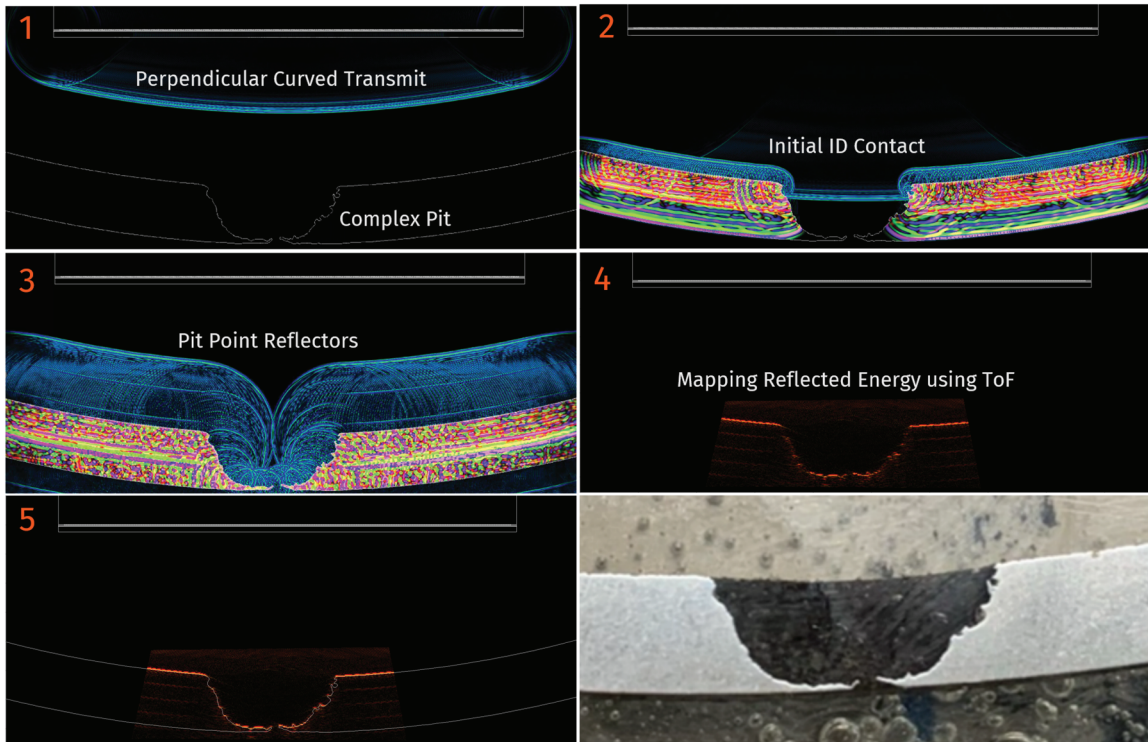
Figure 7: Acoustic Imaging uses diffuse imaging to map a complex and representative through wall pit. [1] Delays are applied electronically to optimize the perpendicularity of the wavefront to match the curvature of the pipe. [2] Initial ID contact, discontinuity clearly apparent in at the pit defect relative to nominal ID. [3] Point reflectors of the complex pit boundary create many spherical wavefronts returning to array. [4,5] TOF delays applied to the amplitude signals used to map the point source reflectors of the pit.

Evaluating Axial Cracks Defects with Acoustic Imaging

High-Resolution Acoustic Imaging addresses the challenges of traditional methods by offering improved spatial mapping of the reflected energy from axial crack-like defects. This approach is particularly differentiated in assessing axial crack defects interacting with SAW and ERW weld seams. Indirect and amplitude-based systems often falter with real crack morphologies that do not closely replicate the idealized EDM notch-based calibration utilized to derive sizing algorithms, creating a delta between performance specifications and real-world outcomes. Techniques like EMAT and conventional UTCD are challenged by slower operational velocities that can impact throughput and hinder their effectiveness in detecting complex crack morphologies, which typically interact with weld seams.

Acoustic imaging has been utilized to accurately size crack-like defects of various types and provides spatial understanding as to the location and identification of the defects in SAW seams as seen in **Figure 8** and in pipe body **Figure 9.**
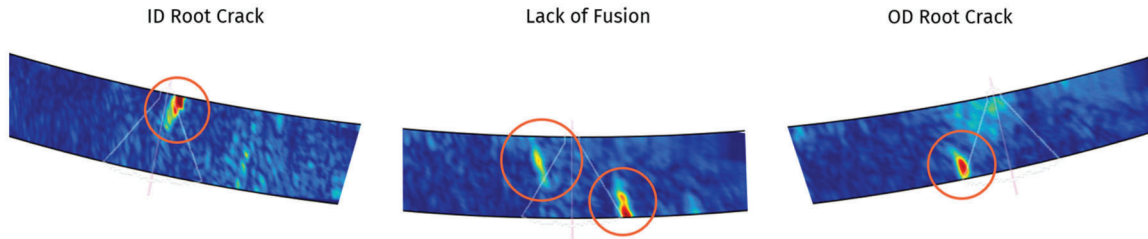

Figure 8: Acoustic Imaging ILI B-scan Examples of different discontinuities in Submerged Arc Weld (SAW) Seams.
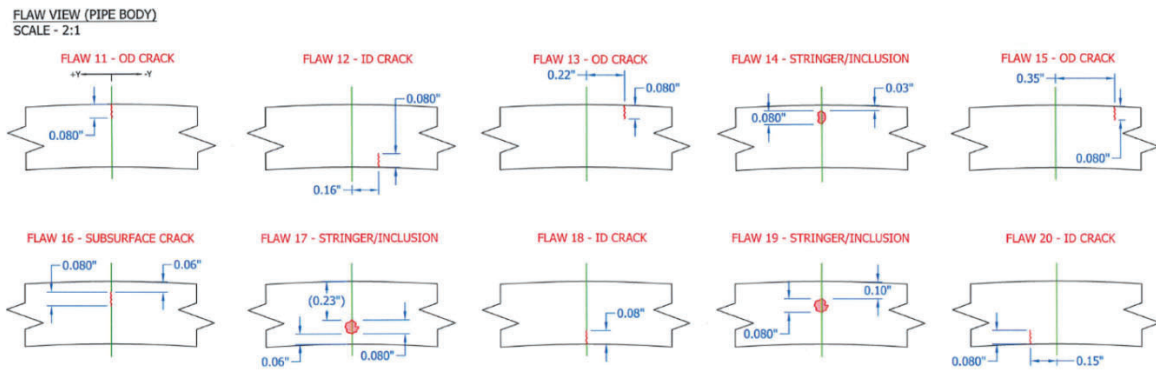
Figure 9: Various types of axial crack-like defects in pipes

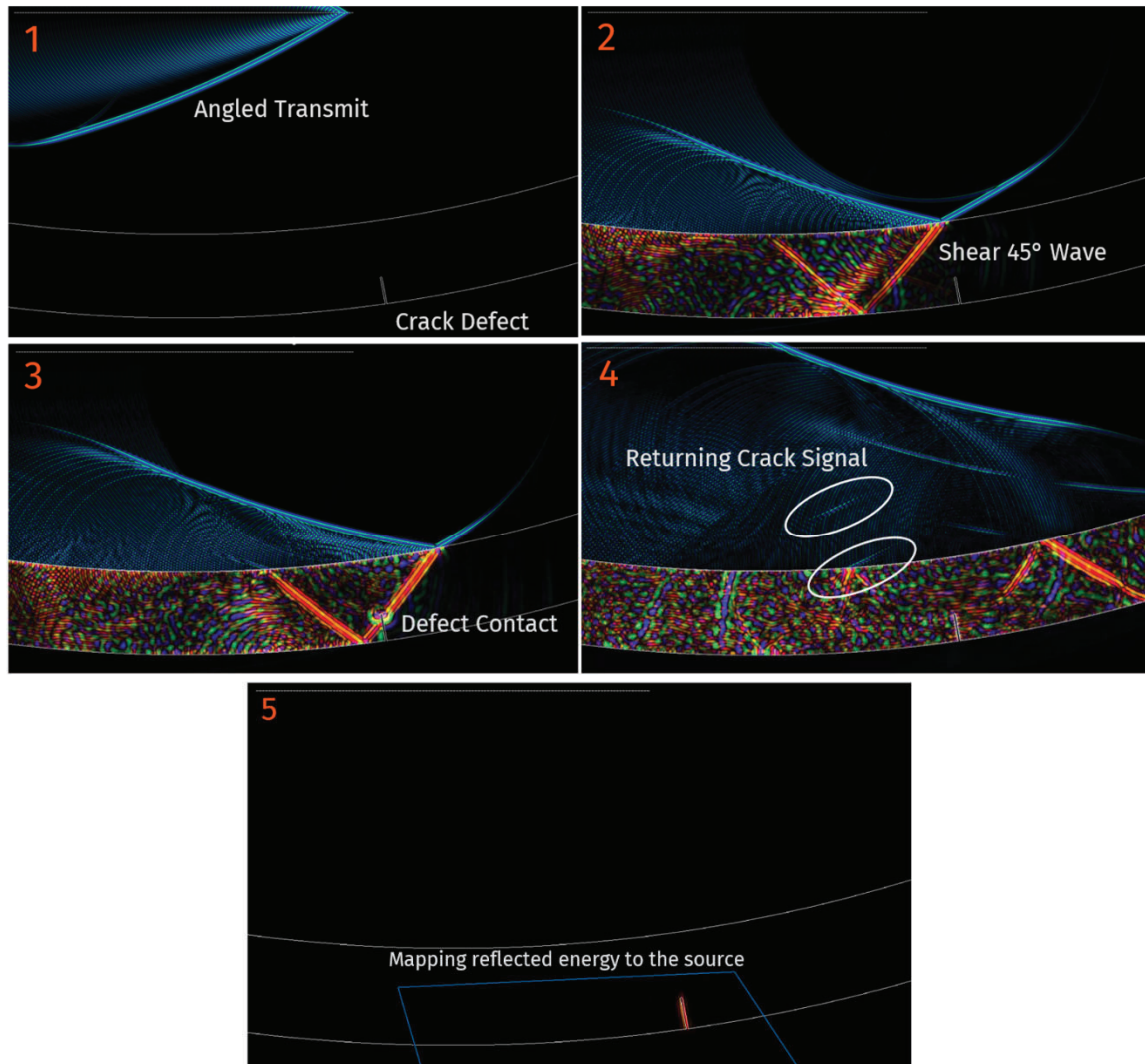## Axial Crack Acoustic Imaging Modes

Angularly steered diverging waves, or steered transmits, are particularly useful for characterizing crack-like defects. By accounting for the returning signal's time-of-flight, direction of propagation, and refraction of the emitted wave on the ID, and its subsequent reflection on the OD, the defect that reflected the energy (or in some cases, lack of energy) can be accurately mapped to its original location. Since the raw data recorded contains all modes of reflection, different wave paths can be reconstructed to offer more information about the defect. **Figure 10** shows some common reflection paths that are analyzed using acoustic imaging [2].
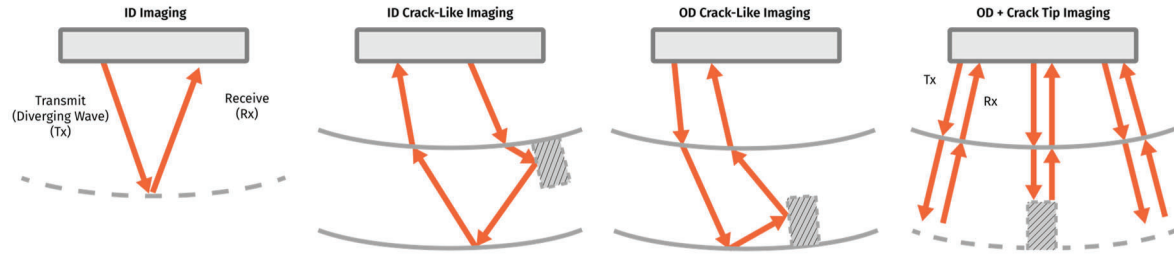
Figure 10: Different signal pathways are used to illuminate different key aspects of a defect. The multipath assessments are captured from the same dataset but are completed by uniquely processing each plausible reflection path. Each brings advantages to improved detection, sizing and identification, and the combined results offer more contextual root cause understanding.

Crack Sizing from Acoustic Imaging

The ability to clearly map the returning energy to a specific component or region within a defect is a novel approach that leverages the full array capture of the acoustic imaging platform as shown in **Figure 11.** Additionally, corrections for the multipath calculations can be refined for the most concerning of defects to account for the precise location of the sensor array relative to the pipe wall. Lastly, the transmit pattern and element sequencing are electronically controlled, meaning that custom imaging sequences can be utilized to mimic sectoral scanning results by indexing through multiple transmit angles. For secondary screening or more highly specialized inspections this means that the imaging can be configured in advance to capture the most elusive crack morphologies.

Figure 11: Acoustic Imaging used to map energy to a slightly off axis or tilted axial crack. [1] Delays are applied electronically to optimize the angle of the approaching wavefront to optimize the penetration of acoustic energy. [2] Initial ID contact, results in the creation of a shear 45-degree wavefront due to the change in speed of sound at the fluid-steel boundary. [3] Shear wave contacts the tilted axial defect; the tip creates a point source reflector while the face of the defect creates a reflector. [4,5] TOF delays applied to the amplitude signals used to map the point source reflectors of the pit.

Acoustic Imaging is not limited by defect indicator saturation or strict calibration requirements commonly experienced in amplitude methods; this makes acoustic imaging techniques robust and reliable across a wide range of defect sizes.

Defects at large tilts and skews are particularly challenging to image using conventional single element based half-skip modes due to the reflections not being captured by the field of view of the probe. To overcome this limitation and leverage the physics of how a tilted or skewed anomaly reflects energy

differently, a shadow-based imaging method is utilized which relies on the shadow created by the defect to size it. A shadow region over the defect is distinctly outlined in the high-density measurements in this mode. Whereas the previously described imaging modalities rely on shear waves, the shadow imaging technique can use either longitudinal waves or shear waves. Longitudinal waves are generated when diverging waves impinge normally on the ID of the pipe, hereinafter referred to as normally-incident transmits.

In addition to creating a shadow, normal transmits also generate crack edge diffractions. When these diffractions are captured at sufficiently high signal-to-noise ratio (SNR), direct modes (see **Figure 10**) can be used to identify the tip and root of crack-like defects with high accuracy. These different imaging modes are then combined to give a clear understanding of the anomaly. From the location of tip and root, users can immediately infer the size and tilt of the crack-like defect. Edge diffractions can appear for both longitudinal and shear wave transmits, but, due to conversion losses, they are generally higher quality with longitudinal waves.
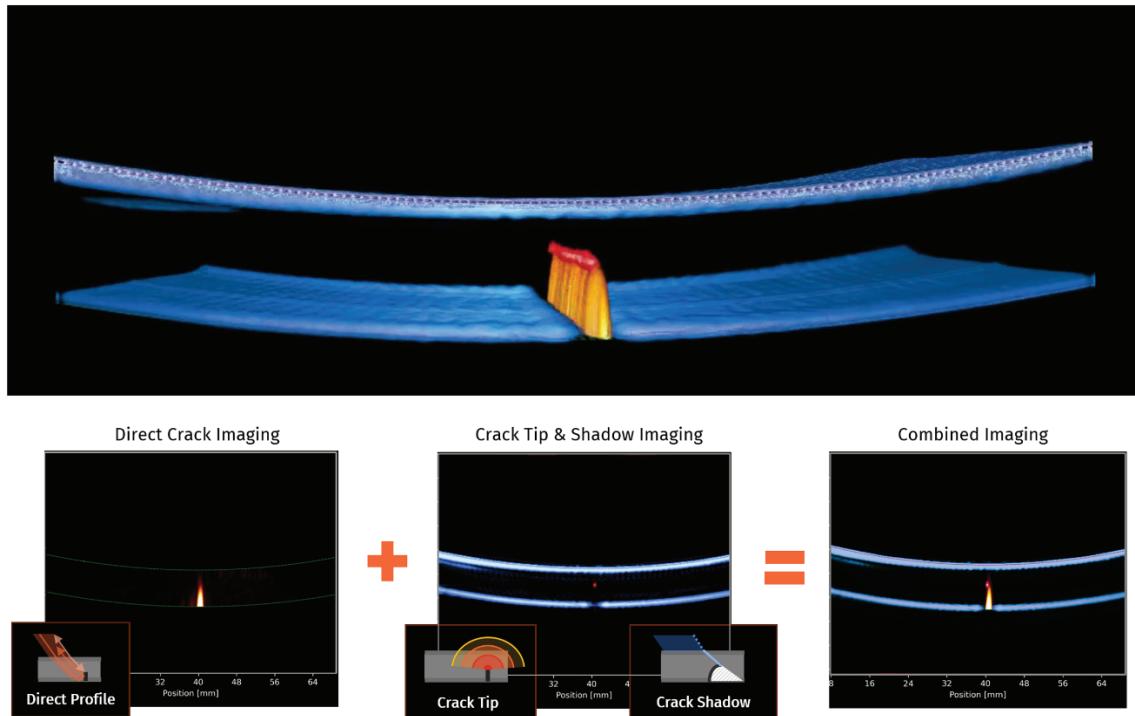

Figure 12: Examples of how different imaging modes are applied to cracks and their resulting output.

Evaluating Dent Defects with Acoustic Imaging

Most validation testing to date has focused on corrosion and cracking, confirming that the system operates within its design and measurement expectations. Ongoing testing and validation, particularly for geometric features, are underway, with more detailed results expected to be released

in 2025. The images in **Figure 13** and **Figure 14** outline some of the early results that have been gained to date validating the base capabilities of dent detection and sizing.
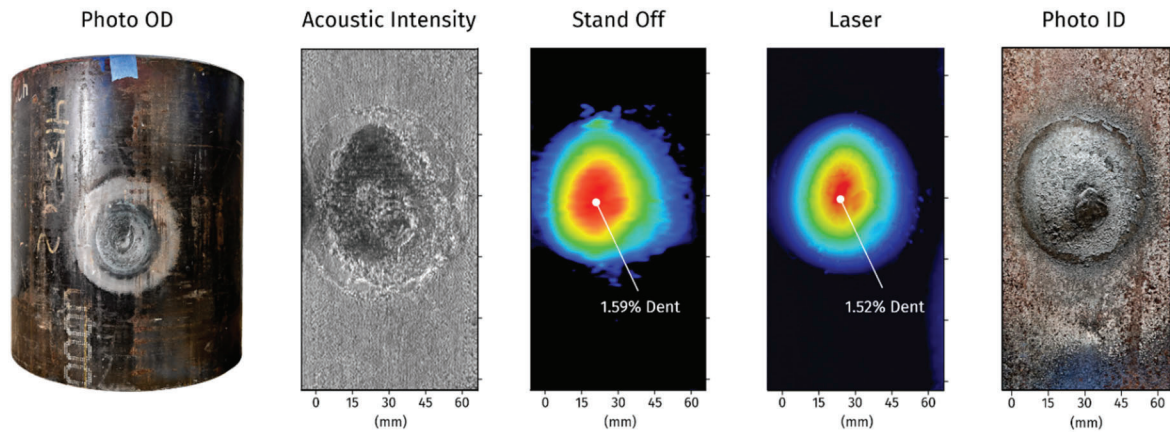
Figure 13: A dent in a pipe sample (far left and right) is evaluated with Acoustic Imaging (2nd and 3rd images) and with a laser scan (2nd right). The Acoustic Intensity view shows the ID texture which can be clearly used as a detection method and the Stand Off view shows the ID displacement measured over the dent from the acoustic ILI tool.
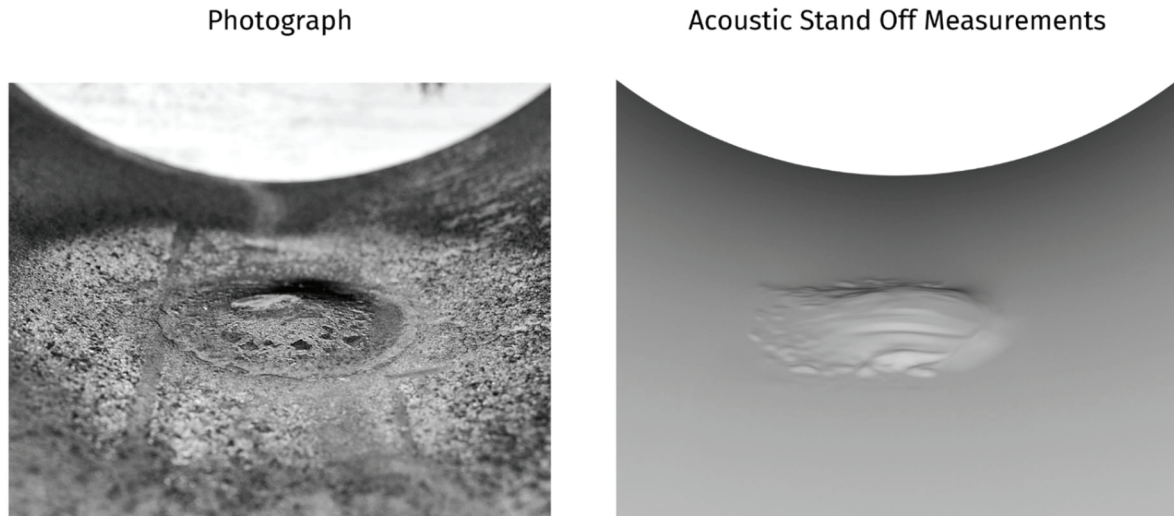
**Figure 14:** Dent geometry is directly measured with the Acoustic Imaging ILI tool and resolves the full contours of the dent.

Validation Results

The Acoustic Imaging technology outlined in this paper is the result of years of rigorous design and validation. Engineering designs and new imaging mode implementations were simulated, prototyped, and progressively tested with increasingly representative conditions.

The validation process involved extensive testing and optimization of both hardware and software systems. Initially, imaging mode parameters were computationally modeled across a wide range of defect types using simulation methods such as ray tracing, and CIVA (an advanced NDT simulation software), while hardware designs were evaluated with Finite Element Analysis (FEA) under various loading conditions.

Once designs and imaging parameters passed the simulation stage, they were physically prototyped and tested to assess their capability to acoustically image and size various defects and samples under diverse conditions. The probes, imaging system, and acquisition parameters were further validated and optimized across different conditions and run speeds in immersion tank setups as seen in **Figure 15.** The Acoustic Imaging acquisition system was integrated with a robotic arm system to enable both axial and circumferential movement, simulating tool motion dynamics along a pipeline in a highly repeatable fashion. This process was iteratively refined across multiple design cycles.
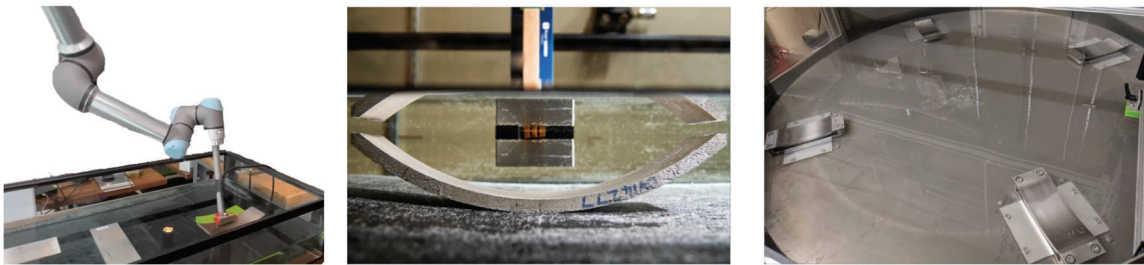
Figure 15: Designs are progressively tested in immersion tanks with increasing representative conditions. Left and center image shows the robotic arm immersion tank in which movement past the same defect can be repeated in a highly controlled manner. Right image shows the turntable immersion tank, in which a variety of defects and mechanical features were traversed at representative line speeds.

API 1163 Detection and Sizing Validation

The API Standard 1163 for assessing ILI systems prescribes that the system's performance be characterized by its ability to detect and size defects. The detection of defects is characterized by the tool's Probability of Detection (POD) and its Probability of Identification (POI). POD is defined as the probability that a feature is detected, and POI is the probability that a feature, once detected, is correctly classified. In this early validation, the API Standard 1163 was applied to assess a statistically significant number of passes and assessments of manufactured notches and flat-bottomed pockets. The defects were varied in length and depth and captured using representative hardware and imaging speeds to obtain early derivation of the tool specifications.

The fully integrated ILI system underwent testing in a newly constructed 1,300ft long continuous-loop test pipeline seen in **Figure 16**. The dedicated, full-scale, infinity loop pipeline, constructed within an indoor facility, enabled comprehensive testing, refinement, and qualification of the complete High-Resolution Acoustic Imaging tool under conditions closely resembling real-world

pipelines. This setup also allows for the evaluation of tool dynamics and wear when passing over common pipeline features such as 3D bends, girth welds, diverters, barred tees, and valves.

The infinity loop has a large spool section in which multiple manufactured features and cutouts from field excavations were flanged and installed to image multiple times over. Testing and validation samples included EDM notches, flat bottom pockets, manufactured flaws, and real field-removed defects. Real and manufactured anomalies include flaws in welds in the toe, root, centerline (both surface breaking and embedded), hook cracks, as well as lack of fusion (LoF), slag inclusion, and porosity. The length, width, and depth of these flaws were assessed.

Each sample was also evaluated with a microCT scan, PAUT, or TFM scans obtained with an Olympus OmniScan X3 performed by a Level III UT technician, or metrology-grade laser scan to provide a reliable ground truth to compare against.
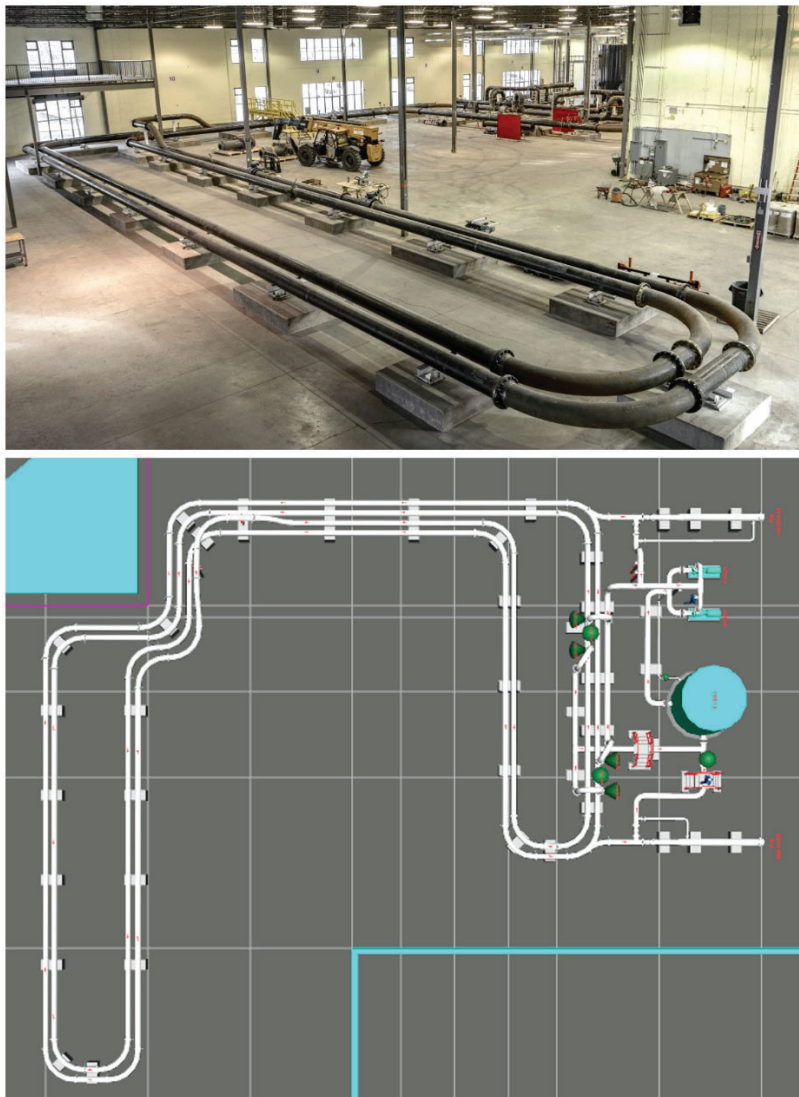
Figure 16: A dedicated full-scale continuously looping test pipeline was constructed in an indoor facility**.**

Validation of Metal Loss Defects

Idealized flat bottom pockets were manufactured in a representative pipe size, material and nominal thickness shown in **Figure 17**. The sample was scanned by the High-Resolution Acoustic Imaging ILI tool to evaluate the overall performance of the technology and the tool.

Figure 17: A machined pipe sample with wall loss defects of varying diameters and various depths used to evaluate POD and sizing accuracy.

The OD flat bottom pocket sample was comprised of an array of idealized OD wall loss defects that ranged in diameter from 25.4 mm down to 1.6 mm. For each diameter of pocket, the depth ranged from 3.1% or 0.4 mm wall loss up to 6.4mm or 50% wall loss as described in **Table 1**. This preliminary study focused on depth range above 12.5% (1.6mm wall loss) or nominal API wall loss specification.

Table 1: Array of OD defects in the flat bottom pocket sample used to evaluate OD wall loss POD and sizing accuracy.

Pocket	Diameter (in)	Diameter (mm)	Depth (in)	Depth (mm)	%Through Wall	Detected?
1	1.00	25.4	0.02	0.4	3.1%	Yes
2			0.03	0.8	6.3%	Yes
3			0.06	1.6	12.5%	Yes
4			0.13	3.2	25.0%	Yes
5			0.19	4.8	37.5%	Yes
6			0.25	6.4	50.0%	Yes
8	0.50	12.7	0.02	0.4	3.1%	Yes
9			0.03	0.8	6.3%	Yes

			0.06	1.6	12.5%	Yes
10			0.06	1.6	12.5%	Yes
11			0.13	3.2	25.0%	Yes
12			0.19	4.8	37.5%	Yes
13			0.25	6.4	50.0%	Yes
15			0.02	0.4	3.1%	Yes
16			0.03	0.8	6.3%	Yes
17	0.25	6.4	0.06	1.6	12.5%	Yes
18			0.13	3.2	25.0%	Yes
19			0.19	4.8	37.5%	Yes
20			0.25	6.4	50.0%	Yes
22			0.02	0.4	3.1%	Yes
23			0.03	0.8	6.3%	Yes
24	0.19	4.8	0.06	1.6	12.5%	Yes
25			0.13	3.2	25.0%	Yes
26			0.19	4.8	37.5%	Yes
27			0.25	6.4	50.0%	Yes
29			0.02	0.4	3.1%	Yes
30			0.03	0.8	6.3%	Yes
31	0.13	3.2	0.06	1.6	12.5%	Yes
32			0.13	3.2	25.0%	Yes
33			0.19	4.8	37.5%	Yes
34			0.25	6.4	50.0%	Yes
36			0.02	0.4	3.1%	No
37			0.03	0.8	6.3%	Yes
38	0.06	1.6	0.06	1.6	12.5%	Yes
39			0.13	3.2	25.0%	Yes
40			0.19	4.8	37.5%	Yes
41			0.25	6.4	50.0%	Yes

The aggregate results from imaging the OD flat bottom pockets are presented below in **Figure 18**, which shows depth sizing across defects with a diameter down to 1.6mm with a preliminary accuracy of +/-0.4mm. The critical conclusion is that deep flaws (>5mm) that have a very small diameter (1.6 mm) footprint are accurately sized owing to the resolution of the acoustic imaging ILI as shown in **Figure 19**. Subsequent studies into small and shallow defects are to be conducted, though in practice, it is noted that deep and small diameter defects or pits are typically a more concerning feature to industry.
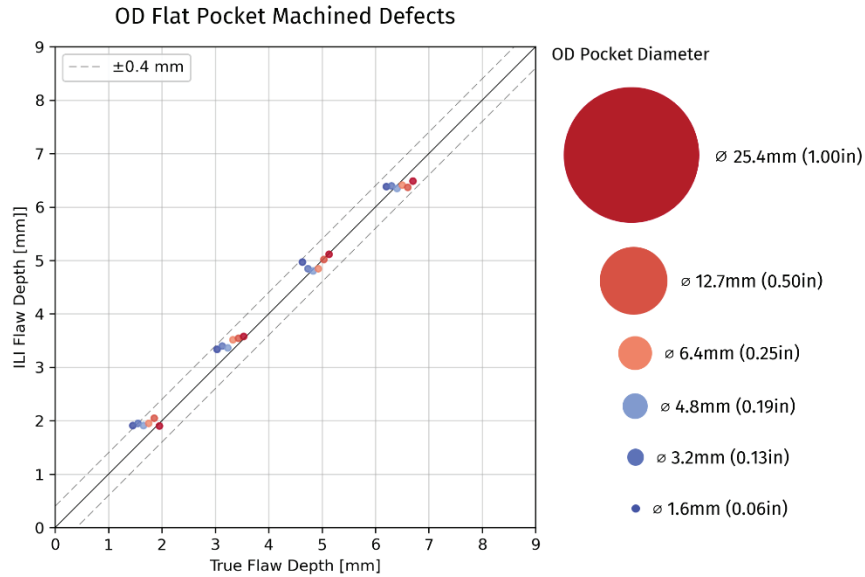
Figure 18: Preliminary Unity Plot of OD Flat Pocket Machined Defects ranging in diameter from 1.6mm to 25.4mm.
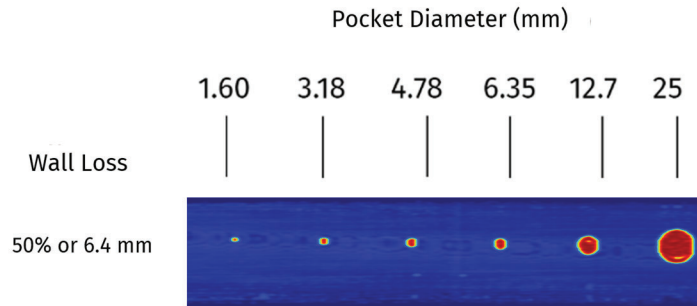
Figure 19: Wall Loss Heatmap of 50% through-wall or 6.4mm deep row of OD pockets ranging in diameter from 25.4 mm (1") to 1.6mm (~1/16")

Validation of Axial Crack-like Defects

Samples with a variety of notches were imaged with EDM notches varying in depth from approximately 0.4mm to 7.0mm and in length from just under 1" (19.5mm) as seen in **Figure 20.** The b-scan results of the amplitude responses received at the tool are presented along with the reference dimensions from the as-built sample. The ability to directly size EDM notch defects is also clearly exhibited, however it's worth noting this behavior is fully expected as these flaws are perfect reflectors and very idealized as compared to real world crack morphologies.
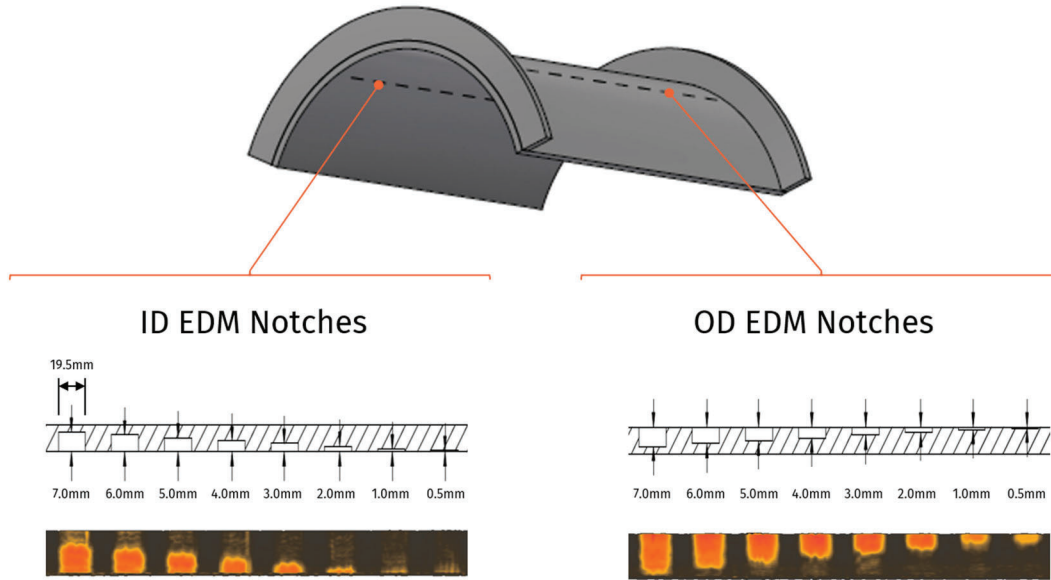
Figure 20: Acoustic Imaging B-scan Visualizations of OD and ID EDM notches cut at varying depths.

As one would expect, with extremely high axial resolution (0.5mm @ 2m/s) the POD for these ˜1" long idealized crack-like EDM manufactured defects was perfect (16/16). This study led to further investigation into the technology's ability to resolve penetrators, which are much shorter flaws that have the potential to be relatively deep.

Validation of Axial Crack Penetrators – Short EDM notches

Additional EDM penetrator sample sets were procured with a typical depth range of 1.6 to 6.3 mm but with very short notch lengths – starting at 5mm and going up to 25.4 mm (1") representing a set of defects entirely below typical industry length thresholds. The resulting length and depth unity plots are shown below in **Figure 21**.
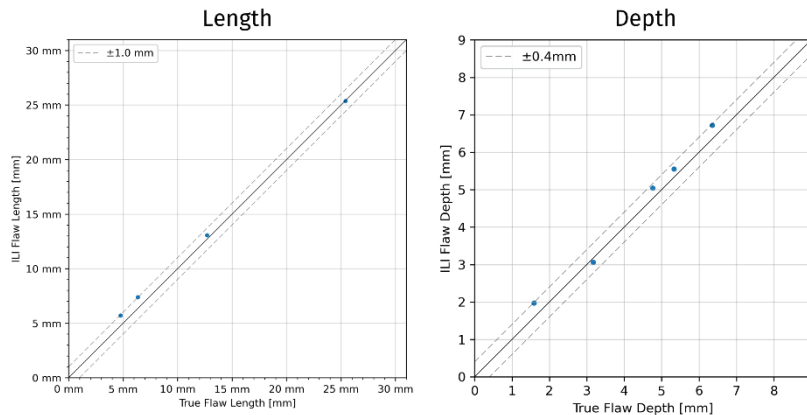
Figure 21: Length and Depth Sizing Unity Plots for <1" length Penetrator EDM notch defects.

Validation of Axial Crack Penetrators – Short Fatigue Crack

In addition to EDM notch samples a more representative crack morphology was assessed to understand the ability to resolve short crack-like defects that currently would go undetected based on today's length thresholds. This defect was also manufactured; however, it relied on fatigue-cycling-based manufacturing methods which resulted in a more natural crack morphology. To assess the "ground truth" length both PAUT handheld device operated by a qualified technician and medical grade CT scanning were used to assess the length accuracy of the acoustic imaging ILI.
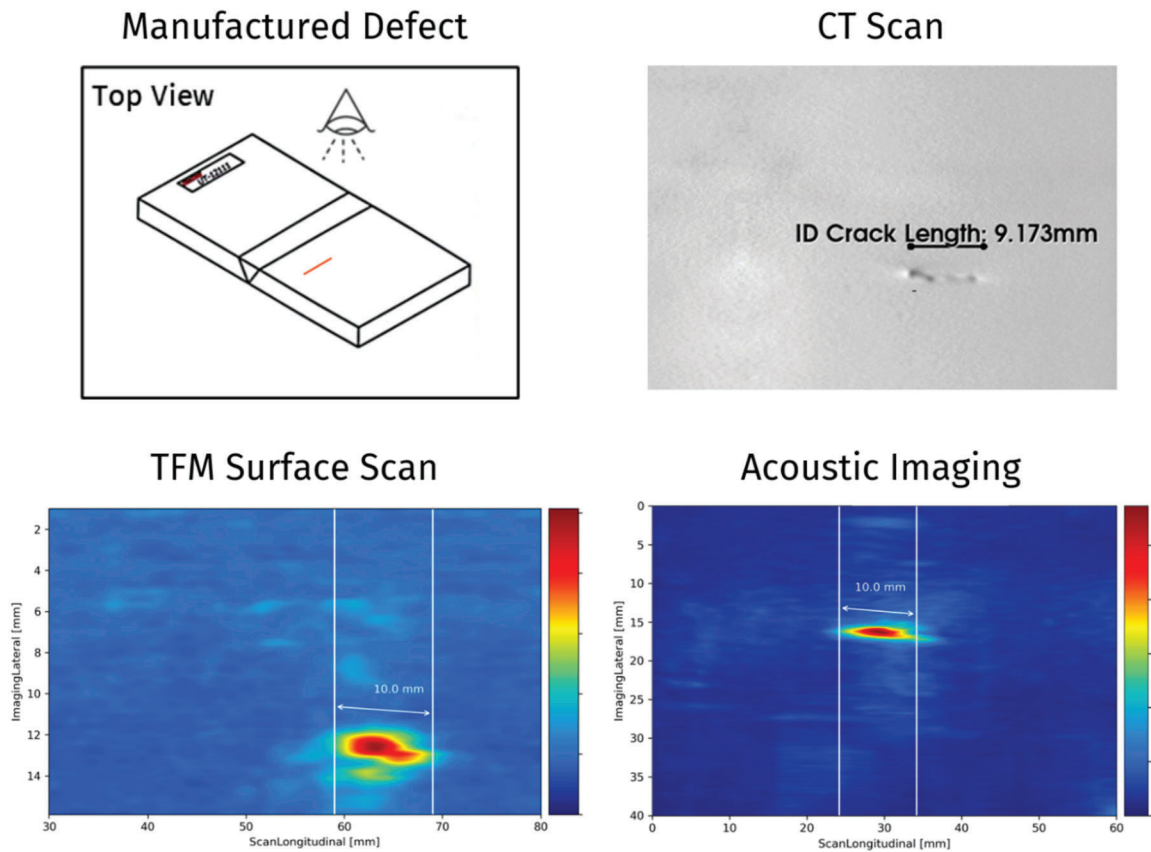

Figure 22: The results from each NDT method show high agreement.

The ground truth methods and Acoustic Imaging ILI tool results showed general agreement in both sizing the depth and length of the defects as seen in **Figure 22.** However, PAUT was not able to properly resolve the geometry of the flaws, and CT struggled to define the extent of certain flaws and cracks due to absorption effects. Both the OmniScan handheld unit and ILI tool were able to clearly discriminate the boundary and geometry of the flaws in the defect samples.

Validation of Axial Crack Penetrators – Short Through Wall LOF Defect Cut Out

After validating representative lab-grown crack morphology, the final assessment of penetrators was a through wall lack of fusion (LOF) defect that was sleeved and ultimately removed from the operating line. This sample was highly complex in that it came from a 1950s vintage ERW pipeline asset. Prior to removal from service this defect had been assessed with high end ILI tools in five separate inspections (2015, 2017, 2019, 2020, 2021, 2022). It was noted that the defect had a low POD due to short length, resulting in outside of specification depth tolerances. The depth sizing through wall percentage from these runs in chronological order was 27%, 29%, 24%, 45% and back down to 29% - none were near the through wall condition that was identified upon digging.

A pull test setup was configured to be able to efficiently assess the defect and optimize imaging parameters if required. The sample was flanged and fluid filled while a stuffing box-type seal was used to pull the ILI hardware past the region of interest.

Figure 23: Through wall-sleeved LOF penetrator defect removed from the pipeline.

The tool was able to locate and confirm the defect to be through wall. The imaging results showed a clean response from a 100% through wall feature as seen in **Figure 24.** This defect was found to be 13 mm in length and confirms the need for higher axial resolution tools capable of detecting significantly shorter-length flaws and sizing them with accuracy. When imaging very deep defects, having a relatively long array of sensors ensures that there is no depth-based amplitude saturation

which can occur in a large single element-based sensor beam. A very deep or through wall defect results in a very wide response signal which can be entirely captured using a wide array-based sensor, so long as the array is acting as independent receiver elements. In addition to assessing the LOF feature, the sleeve's girth welds were also detected – enabling the detection of type B sleeves and confirmation of defect under sleeve. Continued evaluation of this sample is ongoing.
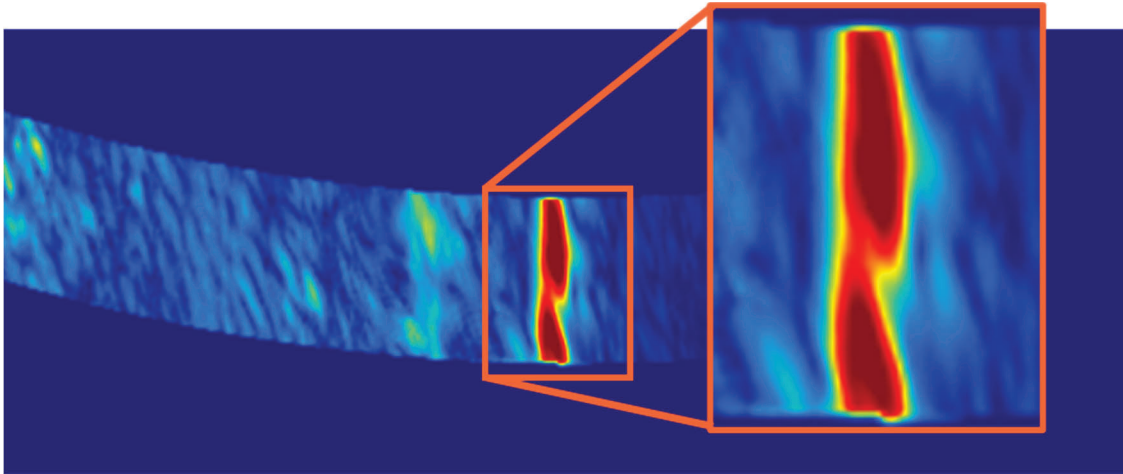
Figure 24: Acoustic Imaging ILI Radial B-scan of through wall-sleeved LOF penetrator defect removed from the pipeline.

Case Study: Field Run with Flint Hills Resources

An inaugural field run was conducted in 2024 along a crude oil pipeline operated by Flint Hills Resources. The High-Resolution Acoustic Imaging tool captured more than 1.7 billion acoustic images and successfully identified and sized multiple instances of pitting and corrosion on the inner diameter (ID) of the pipeline that were compared against dig results.

This field run yielded three important outcomes:
1. The tool performed well within mechanical design expectations and pump track validations.
2. The tool recorded very high quality and high-fidelity data which enabled the identification, sizing, and profiling of pitting and corrosion found in the pipeline.
3. Acoustic Imaging results compared well against NDE in-ditch reports and MFL inspection results from previous inspections of this pipeline.

Pipeline Details

Flint Hills Resources selected a 16-inch pipeline from their system that aligned with the tool's design criteria, serving as an ideal candidate to validate the inspection tool's mechanical capabilities and to field-test its ability to detect and size small internal corrosion and pitting. Being relatively new, this pipeline lacked other threats of concern, such as cracks or dents. Consequently, further validation is planned in other segments to assess the tool's field performance with different types of defects.

<div align="center">Table 2: Key pipeline details:</div>

|	
Length	23.5mi
Wall Thickness	0.375in
Year Installed	2014
Product	Crude
Expected Velocity	3mph
Pressure	200-750 PSI
Seam Type	ERW
Previous Inspections	MFL/Caliper in 2023

Tool Performance

The ILI tool performed very well over the entire length of the pipeline.

- **Velocity** – A steady average velocity of 3mph without speed excursions, surging or stop/starts.
- **Tool Rotation** – The tool gradually rotated approximately 1 rotation every 3mi, ideal for even cup wear and overlapping coverage in the event of sensor channel loss.
- **Tool Pressure (Differential Pressure, DP)** – The tool required 40 psi to move from a static state at the launcher and then ran steadily with 20 psi DP and was fairly constant even while passing through obstacles, such as bends.
- **Battery Performance** – Batteries performed well within the design criteria, only using a small fraction of onboard battery capacity.
- **Internal Temperature** – The tool operated within expected temperature thresholds through the entire run despite the vast computing power required to collect, process and store the significant data generated by the tool.
- **Sensors** – All sensors functioned throughout the run and provided excellent full circumferential coverage of the entire run.
- **Odometer Performance** – Very minimal measurement error across the entire run despite significant wax buildup on wheels of the 6 odometers. Measurements aligned well with the pipe tally. Modifications implemented to reduce wax accumulation.
- **Sensor Arm Standoff** – Sensor carrier arms performed well and contributed to high-quality data acquisition over sudden geometry changes like girth welds, deformations, offsets, and step changes.

Imaging Performance: Wall Loss

There was particular interest in the early detection, sizing, and monitoring of the growth of small pitting wall loss in this line. These pitting defects have been challenging to identify early due to the small features often falling under the detection abilities of legacy inspection technologies.

This run demonstrates the High-Resolution Acoustic Imaging tool's ability to identify and measure pitting or other corrosion anomalies before they become hazardous. **Figure 25** shows ID pitting in 3D that was created from the dense point cloud measurements from Acoustic Imaging. A locally projected cross-sectional view at the base of the figure highlights the varying pit depths and wall loss across the length of the pipe.
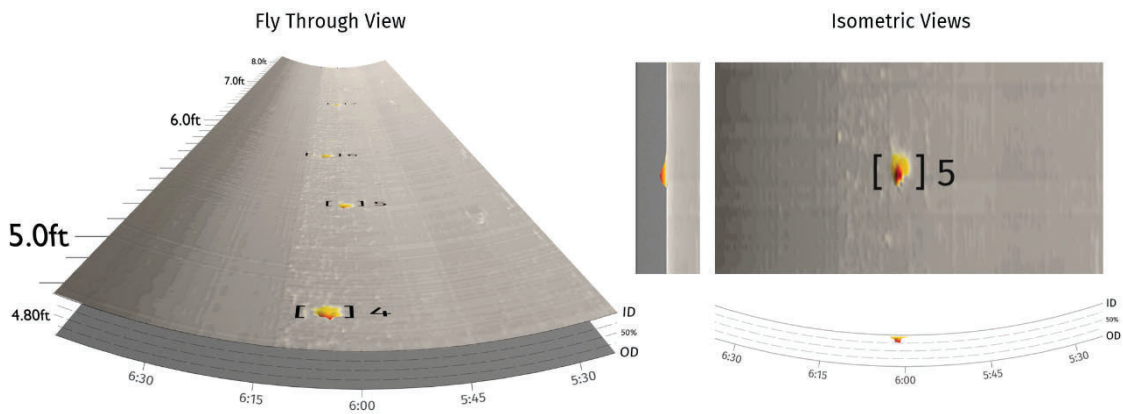
Figure 25: A detailed surface map of the defects found and sized is created with Acoustic Imaging.

The resolving ability and intuitive visualization of the pitting in 3D detail helped the operator understand the severity and characteristics of the pitting. The sharp edges of the pits were clearly identified and enabled the operator to narrow in on the root cause of the pitting defects.

Comparison with NDE and MFL for Evaluating Wall Loss

The availability of a recent magnetic flux leakage (MFL) axial field inspection and corresponding dig results provided an excellent opportunity to evaluate the performance of the Acoustic Imaging tool against existing industry technologies.

In general, there was a strong agreement between the NDE data and High-Resolution Acoustic Imaging results. The MFL tool performed roughly within specifications, but it shows a consistent undersizing of the pitting defects when compared to the NDE measurements. The Acoustic Imaging results showed a much tighter agreement with the NDE results. **Figure 26** and **Table 3** below show the differences between the three technologies across the defects inspected.
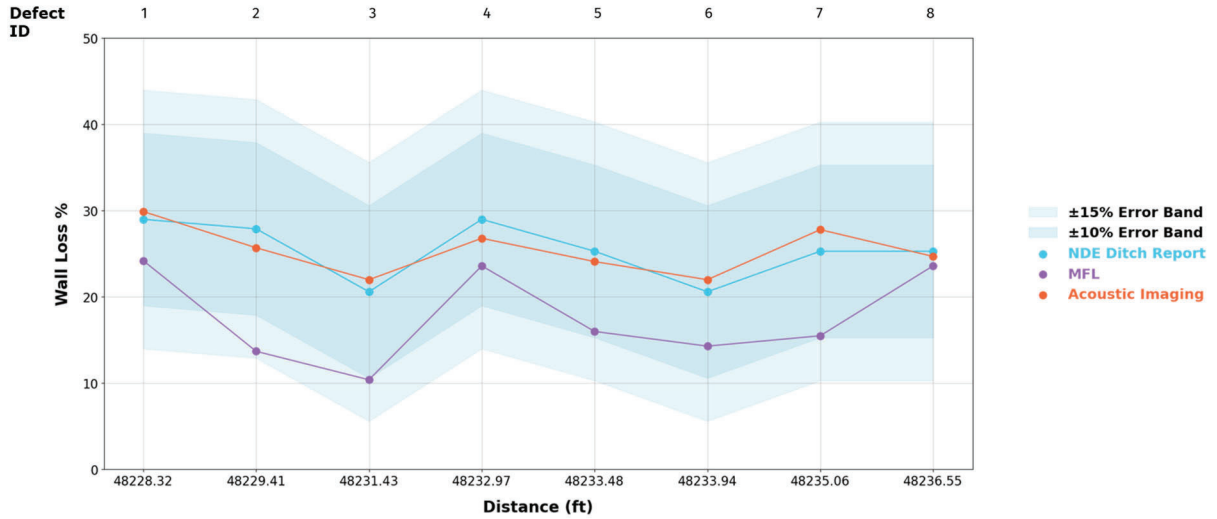
Figure 26: Acoustic Imaging (orange) and MFL (purple) tool results compared to NDE (blue) results over multiple defects.

The following table compares results from multiple defects where NDE in the ditch is assumed to be ground truth.

Table 3: Comparison of Acoustic Imaging ILI and previously ran MFL relative to the NDE results from in-ditch assessments.

| Defect ID	1	2	3	4	5	6	7	8
Acoustic Imaging vs. NDE	0.9%	-2.2%	1.4%	-2.2%	-1.2%	1.4%	2.5%	-0.6%
MFL vs. NDE	-4.8%	-14.2%	-10.2%	-5.4%	-9.3%	-6.4%	-9.8%	-1.7%

Acoustic Imaging Compared to Dig Results

Results from both Acoustic Imaging and MFL are plotted against NDE results as seen in **Figure 27**. These unity plots illustrate the lower error bounds of the Acoustic Imaging tool and its ability to accurately size defects.
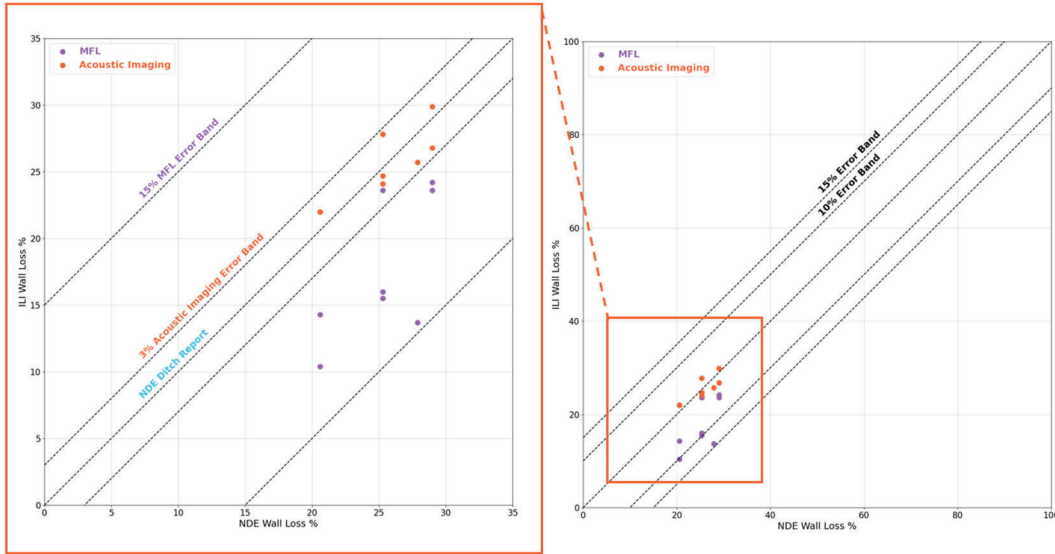
Figure 27: A unity plot of the defects reported by an MFL tool and Acoustic Imaging tool compared to in-ditch surface measurements. The MFL results show systemic under-call bias with an ˜15% error. The Acoustic imaging results are evenly distributed around unity with a +/- 3% accuracy.

Field non-destructive evaluation (NDE) measurements done in the ditch, obtained using technologies such as TFM, are widely regarded as highly reliable for evaluating internal diameter (ID) defects in pipelines. However, in certain cases, particularly with pitting, the resolution of NDE reports can be limited, as the shapes are often depicted with only a few pixels, making precise contour and depth assessments challenging. In contrast, Acoustic Imaging provides a high-resolution 3D profile, allowing for clear visualization and accurate measurement of the pit's exact contours and depth as seen in **Figure 28**.

NDE Wall Loss	20.6%
Acoustic Imaging Wall Loss	22.0%

NDE
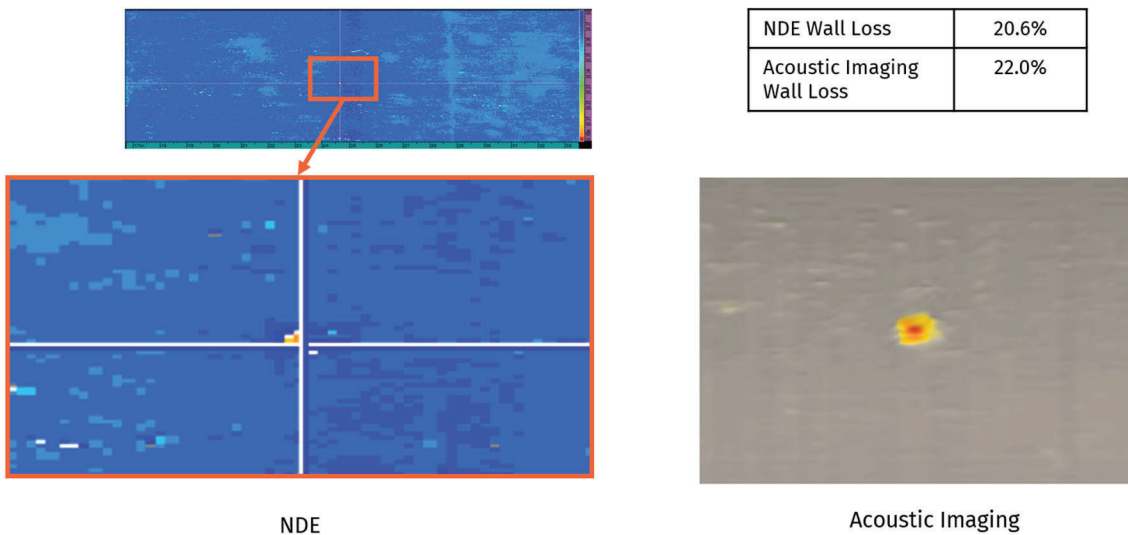
Acoustic Imaging

Figure 28: A side-by-side comparison of the resolution and defect-resolving ability of the ground truth NDE method vs the Acoustic Imaging method.

Conclusions

This novel High-Resolution Acoustic Imaging technology deployed in an ILI tool has been shown to offer measurably improved inspection capabilities over a wide range of anomaly types.

- The tool has demonstrated high-resolution capabilities to simultaneously evaluate metal loss, cracks, and dents at 0.25mm circumferential resolution and 0.5mm axial and at 2 meters/second inspection speed.
- The tool has been proven in the field and in full-scale crude oil pipeline runs to be highly robust while performing well within its design parameters and capable of navigating common pipeline obstacles.
- Results from the field runs of the acoustic imaging ILI tool aligned much closer to NDE reported sizes over prior ILI MFL reported results, which significantly and systemically under-called the population of ID pitting features.
- The smallest pinhole and corrosion-like defect detected and sized to date by the tool was 1.6mm in diameter. This diameter pinhole was accurately depth-sized for depths ranging from 0.8mm to 6.4mm in depth. Additional test loop validation work is ongoing to quantify small diameter and shallow pinhole and pitting flaws.
- The shortest crack-like defect detected and sized to date by the tool was 5mm in length. This length of crack-like defect was accurately sized from 1.6mm up to 6.4 in depth. Additional test loop validation work is ongoing to quantify short and shallow crack-like flaws.
- The phased array-based architecture operates each element entirely independently, resulting in extremely high-density coverage and fidelity. Each array is sequenced electronically using proprietary electronics and software to steer each acoustic beam clockwise, counterclockwise and normal to the pipe. These wavefronts are curved to match the pipe wall profile, maximizing the amount of energy entering the pipe wall.
- The application of multiple post-run direct imaging modes provides enhanced inspection results and contextual understanding of defects and anomalies. Each imaging mode highlights features such as crack-tips, shadows of flaws, surface texture and weld cap geometries. The resulting images can be synthesized into highly insightful renderings providing contextual understanding of the region which can aid in the dig selection process.
- The visualizations from the technology reduces subjectivity and biased interpretation of results, providing a deeper understanding of defects beyond size metrics.

This paper marks the introduction of High-Resolution Acoustic Imaging into the midstream industry to address the challenges faced with existing solutions. Ongoing validation testing and field testing are scheduled to further evaluate the tool performance across a full variety of defects, including wall loss, cracks, deformations, and complex corrosion on both internal and external surfaces.

References

American Petroleum Institute (API). API 1163 In-Line Inspection Systems Qualification (Second Edition, April 2013)

Robinson, S., Littleford, T., Luu, T., et al. 2020. Acoustic Imaging of Perforation Erosion in Hydraulically Fractured Wells for Optimizing Cluster Efficiency. Presented at the SPE Hydraulic Fracturing Technology Conference and Exhibition, Texas, https://doi.org/10.2118/199718-MS

Holmes, C., Drinkwater, B. W., & Wilcox, P. D. (2005). Post-processing of the full matrix of ultrasonic transmit–receive array data for non-destructive evaluation. *NDT & E International*, *38*(8), 701–711. https://doi.org/10.1016/j.ndteint.2005.04.002

Felice, M. V., & Fan, Z. (2018). Sizing of flaws using ultrasonic bulk wave testing: A review. *Ultrasonics*, *88*, 26–42. https://doi.org/10.1016/j.ultras.2018.03.003

Simpson, G., T. Littleford, and A. Battistel, 2022, High-Resolution Acoustic Imaging for Submillimetric Casing Thickness Quantification and Advanced Effective-Area-Based Burst Pressure Analyses. https://doi.org/10.2118/210010-MS

B. E. Treeby, J. Jaros, D. Rohrbach, and B. T. Cox, "Modelling elastic wave propagation using the k-Wave MATLAB toolbox," IEEE International Ultrasonics Symposium, pp. 146-149, 2014.